

Antenna Position Estimation Through Sub-Sampled Exponential Analysis of Harmonically Related Input Signals

Ridalise Louw^{*(1)}, Ferre Knaepkens⁽²⁾, Annie Cuyt⁽²⁾⁽³⁾, Wen-shin Lee⁽⁴⁾⁽²⁾, Stefan J. Wijnholds⁽⁵⁾⁽¹⁾, Dirk I. L. de Villiers⁽¹⁾, Rina-Mari Weideman⁽¹⁾

(1) Department of Electrical and Electronic Engineering, Stellenbosch University, Stellenbosch, South Africa

(2) Department of Computer Science, University of Antwerp, Middelheimlaan 1, 2020 Antwerpen, Belgium

(3) College of Mathematics and Statistics, Shenzhen University, Shenzhen, Guangdong 518060, China

(4) Division of Computing Science and Mathematics, University of Stirling, Stirling FK9 4LA, Scotland (UK)

(5) Netherlands Institute for Radio Astronomy (ASTRON), Dwingeloo, The Netherlands

Abstract

Accurate placement of elements in large antenna arrays is a difficult and costly process. We explore the use of the validated exponential analysis (VEXPA) technique that was previously formulated to solve a direction-of-arrival (DOA) estimation problem, to find the antenna element positions in an array after the installation phase, so that cost-savings can be realised during placement of the antenna elements. Measurements are taken from harmonically related input signals transmitted from an Unmanned Aerial Vehicle (UAV) for which the position in the sky is known. It is shown how the UAV's zenith angle can be manipulated to generate parameters required for VEXPA's de-aliasing step. A simple simulation illustrates the functioning of the proposed method.

1 Introduction

Accurate beamforming of an array of antennas requires accurate knowledge of the positions of the individual antennas. Establishing those antenna positions can be an elaborate process for large-N radio interferometers like the Low Frequency Array (LOFAR) [1] and the Square Kilometre Array (SKA) [2]. In [3], a method was proposed to measure the positions of the individual antennas using an Unmanned Aerial Vehicle (UAV). As this is done after installation, it facilitates a more cost-effective roll-out of the antennas by being tolerant to antenna placement errors and errors when connecting the antennas to the back-end. In this contribution, we recognise that these UAV measurements can actually be considered as an inverse-DOA estimation problem and explore the possibility to use the exponential analysis method developed for DOA estimation in [4] for antenna position estimation.

2 Problem Formulation

Figure 1 illustrates the odd harmonic signals $S_i(t)$ transmitted from the UAV located at zenith and azimuth angles, θ and ϕ , respectively. The index $i \in \mathbb{N}$ is a range of natural numbers that is used to distinguish between narrow-

band signals at different odd harmonic frequencies $\omega_i = 2(i + \frac{1}{2})\omega_0$, with ω_0 the base frequency. At a time t the

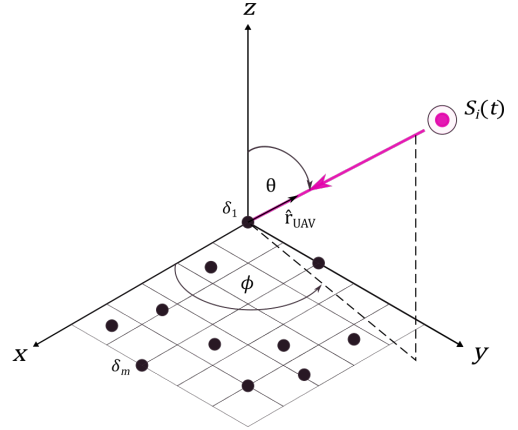


Figure 1. Illustration of signals $S_i(t)$ transmitted from the UAV towards a planar array.

signals are expressed as

$$S_i(t) = s_i(t) \exp(j\omega_i t) \quad (1)$$

where $s_i(t) = a_i(t) \exp(jp_i(t))$ and the slowly varying amplitude and phase of the signal are denoted by $a_i(t)$ and $p_i(t)$, respectively. It is assumed that this signal is strong enough so that astronomical sources in the field of view of the array can be ignored, as in [3]. For large arrays, the source is in the radiating near-field of the antenna, thus a curved phase front is incident on the array. A possible solution for this is to estimate the positions of elements in the array incrementally using a subset of antennas to ensure the far-field condition. For purposes of illustration, the far-field condition is assumed, such that $S_i(t)$ is a plane wave incident on the array.

The first element is chosen to coincide with the origin, i.e., $\delta_1 = (0, 0)$. The time delay of incidence on the m_{th} antenna element at a position $\delta_m = (\delta_{mx}, \delta_{my})$ on the

$x - y$ grid relative to δ_1 is given by

$$\begin{aligned}\tau_m &= \frac{\hat{\mathbf{r}}_m \cdot \hat{\mathbf{r}}_{\text{UAV}}}{c} \\ &= \frac{\delta_{mx} \sin \theta \cos \phi + \delta_{my} \sin \theta \sin \phi}{c},\end{aligned}\quad (2)$$

where $\hat{\mathbf{r}}_m = \delta_{mx}\hat{\mathbf{x}} + \delta_{my}\hat{\mathbf{y}} + (0)\hat{\mathbf{z}}$ is the position of the m th antenna element in the (x, y) -plane, $\hat{\mathbf{r}}_{\text{UAV}} = \sin \theta \cos \phi \hat{\mathbf{x}} + \sin \theta \sin \phi \hat{\mathbf{y}} + \cos \theta \hat{\mathbf{z}}$ is the unit vector from the origin to the UAV's position (θ, ϕ) and c is equal to the propagation velocity of the signal, or in free space, the speed of light. The narrowband assumption that the signal does not change noticeably as it moves across the elements of the array gives an output at the m th antenna element at time t for frequency i as

$$\begin{aligned}f_{mi}(t) &= S_i(t + \tau_m) \\ &\approx s_i(t) \exp(j\omega_i t) \exp(j\omega_i \tau_m) \\ &= S_i(t) \exp\left(j \frac{\omega_i}{c} \hat{\mathbf{r}}_m \cdot \hat{\mathbf{r}}_{\text{UAV}}\right).\end{aligned}\quad (3)$$

2.1 Element Data Model

To extract the two-dimensional element positions $(\delta_{mx}, \delta_{my})$, we require signals from two linearly independent directions in a plane parallel to the (x, y) -plane [5]. Let the first direction $\Delta_1 = \cos \phi_1 \hat{\mathbf{x}} + \sin \phi_1 \hat{\mathbf{y}}$ and the second direction $\Delta_2 = \cos \phi_2 \hat{\mathbf{x}} + \sin \phi_2 \hat{\mathbf{y}}$. The common factor $\sin \theta$ is intentionally excluded in these definitions, as it is used in the following section to model the sub-sampled exponential analysis problem. Then at a fixed time t , we use the following shorthand notations:

$$\begin{aligned}f_{mi} &= f_{mi}(t), \\ \alpha_i &= s_i(t), \\ \beta_i &= S_i(t) = \alpha_i \exp(j\omega_i t), \\ \Psi_{m1} &= j \frac{\omega_0}{c} \sin \theta (\delta_{mx} \cos \phi_1 + \delta_{my} \sin \phi_1), \\ \Psi_{m2} &= j \frac{\omega_0}{c} \sin \theta (\delta_{mx} \cos \phi_2 + \delta_{my} \sin \phi_2).\end{aligned}\quad (4)$$

We distinguish between the coefficients α_{i1} and α_{i2} for the different flight paths of the UAV along Δ_1 and Δ_2 . Then $\beta_{i1} = \alpha_{i1} \exp(j\omega_i t)$ and $\beta_{i2} = \alpha_{i2} \exp(j\omega_i t)$. The samples collected at each element m are filtered into sub-bands, thus for the two different directions we have

$$\begin{aligned}f_{mi1} &= \beta_{i1} \exp\left(2\left(i + \frac{1}{2}\right) \Psi_{m1}\right), \\ f_{mi2} &= \beta_{i2} \exp\left(2\left(i + \frac{1}{2}\right) \Psi_{m2}\right).\end{aligned}\quad (5)$$

The coefficients β_i depend on the different frequencies ω_i . This is undesirable, so a pre-processing step is to mix all signals down to DC through digital multiplication of $\exp(-j\omega_i t')$ at each corresponding sub-band, where t' indicates a time different to t . A constant phase component remains in each case, denoted as $\exp(j\omega_i \Delta_{T1})$ and $\exp(j\omega_i \Delta_{T2})$, where Δ_{T1} and Δ_{T2} refer to the time difference $t - t'$ corresponding to each case. This is dealt with

by realising that the reference antenna element's position $\delta_1 = (0, 0)$ and at time $t = 0$:

$$f_{1i}(0) = s_i(0) \exp(j\omega_i \Delta_T) \exp(0) \quad (6)$$

which is some constant for both directions Δ_1 and Δ_2 that can be normalised to 1. We can therefore remove the varying phase offsets by dividing all mixed down sample sets that are collected at different time intervals with the mixed down value of the first sample in time for the first antenna element f_{1i} . The samples in both directions then become:

$$\begin{aligned}f'_{mi1} &= \frac{\alpha_{i1} \exp(j\omega_i \Delta_{T1}) \exp\left(2\left(i + \frac{1}{2}\right) \Psi_{m1}\right)}{f_{1i1}(0)} \\ &= \exp\left(2\left(i + \frac{1}{2}\right) \Psi_{m1}\right), \\ f'_{mi2} &= \frac{\alpha_{i2} \exp(j\omega_i \Delta_{T2}) \exp\left(2\left(i + \frac{1}{2}\right) \Psi_{m2}\right)}{f_{1i2}(0)} \\ &= \exp\left(2\left(i + \frac{1}{2}\right) \Psi_{m2}\right).\end{aligned}\quad (7)$$

It is interesting to note that these phases are equal to the phases of the correlations measured on the equivalent base-lines between element m and the element at the origin.

2.2 Sub-Sampled Exponential Analysis

Let λ_0 denote the wavelength corresponding to the base frequency ω_0 . Then, if the spatial Nyquist criteria

$$|\sin \theta (\delta_{mx} \cos \phi_1 + \delta_{my} \sin \phi_1)| < \frac{\lambda_0}{2} \quad (8a)$$

$$|\sin \theta (\delta_{mx} \cos \phi_2 + \delta_{my} \sin \phi_2)| < \frac{\lambda_0}{2}, \quad (8b)$$

are not met for all antenna element positions δ_m , we are dealing with a sub-sampled exponential analysis problem that can be solved by using the VEXPA technique described in [6]. VEXPA's de-aliasing method makes use of co-prime scale and shift parameters σ and ρ , respectively. The UAV's zenith angle θ can be exploited to model these parameters. First define a virtual wavelength

$$\lambda_v > \lambda_0 \quad (9)$$

large enough to ensure that the spatial Nyquist criteria

$$|\delta_{mx} \cos \phi_1 + \delta_{my} \sin \phi_1| < \frac{\lambda_v}{2} \quad (10a)$$

$$|\delta_{mx} \cos \phi_2 + \delta_{my} \sin \phi_2| < \frac{\lambda_v}{2} \quad (10b)$$

are met for all m antenna element positions. Then, define

$$\begin{aligned}\Phi_{m1} &= j \frac{\omega_v}{c} (\delta_{mx} \cos \phi_1 + \delta_{my} \sin \phi_1) \\ \Phi_{m2} &= j \frac{\omega_v}{c} (\delta_{mx} \cos \phi_2 + \delta_{my} \sin \phi_2),\end{aligned}\quad (11)$$

where the virtual frequency $\omega_v = \frac{2\pi c}{\lambda_v}$.

We need to collect the following samples at each antenna element m :

$$f'_{m(i\sigma)_1} = \exp\left(\sigma\left(i + \frac{1}{2}\right)\Phi_{m1}\right) \quad (12a)$$

$$f'_{m(i\sigma+\rho)_1} = \exp\left(\left(\sigma\left(i + \frac{1}{2}\right) + \rho\right)\Phi_{m1}\right) \quad (12b)$$

$$f'_{m(i\sigma)_2} = \exp\left(\sigma\left(i + \frac{1}{2}\right)\Phi_{m2}\right) \quad (12c)$$

$$f'_{m(i\sigma+\rho)_2} = \exp\left(\left(\sigma\left(i + \frac{1}{2}\right) + \rho\right)\Phi_{m2}\right). \quad (12d)$$

To do this, let θ_σ denote the zenith angle of the UAV during collection of the samples in (12a) and (12c). From comparison with (7) we have

$$\sigma\left(i + \frac{1}{2}\right)\omega_v = 2\left(i + \frac{1}{2}\right)\omega_0 \sin \theta_\sigma, \quad (13)$$

so that

$$\sin \theta_\sigma = \frac{\sigma\omega_v}{2\omega_0}. \quad (14)$$

The left hand side of (13) is the desired model and the right hand side is the description of what is physically going on. The angle θ_σ is calculated from the scale parameter $\sigma \in \mathbb{Q}$. It is not a requirement for σ (or θ_σ) to have the same value in both directions Δ_1 and Δ_2 , but this is done to simplify the analysis. The UAV's zenith angles θ_{ρ_i} during collection of the samples in (12b) and (12d) are calculated from the shift parameter $\rho \in \mathbb{Q}$ and once again comparing with (7):

$$\left(\sigma\left(i + \frac{1}{2}\right) + \rho\right)\omega_v = 2\left(i + \frac{1}{2}\right)\omega_0 \sin \theta_{\rho_i}, \quad (15)$$

such that

$$\sin \theta_{\rho_i} = \frac{\left(\sigma\left(i + \frac{1}{2}\right) + \rho\right)\omega_v}{2\left(i + \frac{1}{2}\right)\omega_0}. \quad (16)$$

The values of $\sigma, \rho \in \mathbb{Q}$ must be chosen as coprime and lead to sensible values for the angles $\theta_\sigma, \theta_{\rho_i}$. Notice that the UAV's flight path should include $2(n+1)$ positions leading to signal DOAs of $(\phi_1, \theta_\sigma), (\phi_1, \theta_{\rho_i}), (\phi_2, \theta_\sigma)$, and $(\phi_2, \theta_{\rho_i})$, where n is the number of frequency harmonics transmitted.

From the samples in (12) we can solve each antenna element's position δ_m relative to δ_1 . We collect N_t time samples, also known as snapshots, at different time intervals for each base term in (12). We then calculate N_t scaled base terms $\exp(\sigma\Phi_{m1})$ and $\exp(\sigma\Phi_{m2})$ with the Root-MUSIC algorithm [7], which requires a time average of the samples at each antenna for the different frequencies in order to approximate the covariance matrix. For this purpose, we use a subset of $N_s < N_t$ randomly chosen sub-snapshots for each of the N_t evaluations of Root-MUSIC.

Note from (12) that the base terms $\exp(\rho\Phi_{m1})$ and $\exp(\rho\Phi_{m2})$ are the coefficients of the shifted samples. These are solved in the least squares sense for each antenna element at each snapshot separately in both directions from the respective Vandermonde systems

$$\begin{bmatrix} 1 \\ \exp(\sigma\Phi_m) \\ \vdots \\ \exp((n-1)\sigma\Phi_m) \end{bmatrix} \exp(\rho\Phi_m) = \begin{bmatrix} f'_{m(\sigma+\rho)} \\ \vdots \\ f'_{m((n-1)\sigma+\rho)} \end{bmatrix}, \quad (17)$$

with n the number of frequency harmonics, ω_i .

As a result of noise, the N_t evaluations of $\exp(\sigma\Phi_{m1})$, $\exp(\rho\Phi_{m1})$, $\exp(\sigma\Phi_{m2})$ and $\exp(\rho\Phi_{m2})$ are clustered around the true solution in the complex plane. To locate our best estimate of these base terms, we do a search for the densest point among the possible N_t points. The densest point has a specified minimum number of points around it within the smallest possible radius.

We then have two sets of possible solutions for each direction:

$$\left\{ \exp\left(\Phi_{m1} + \frac{j2\pi}{\sigma}l\right) : l = 0, \dots, \sigma - 1 \right\}, \quad (18)$$

$$\left\{ \exp\left(\Phi_{m1} + \frac{j2\pi}{\rho}l\right) : l = 0, \dots, \rho - 1 \right\}$$

and

$$\left\{ \exp\left(\Phi_{m2} + \frac{j2\pi}{\sigma}l\right) : l = 0, \dots, \sigma - 1 \right\}, \quad (19)$$

$$\left\{ \exp\left(\Phi_{m2} + \frac{j2\pi}{\rho}l\right) : l = 0, \dots, \rho - 1 \right\}.$$

Since σ and ρ are chosen to be coprime, the intersection of the sets in (18) contains only one root which is the unique solution $\exp(\Phi_{m1})$, and similarly, the intersection of the sets in (19) gives the unique solution for $\exp(\Phi_{m2})$ [8]. Thus the aliasing problem is solved.

Since the vectors Δ_1 and Δ_2 are linearly independent, the 2×2 regular linear system

$$j\frac{\omega_v}{c} \begin{bmatrix} \cos \phi_1 & \sin \phi_1 \\ \cos \phi_2 & \sin \phi_2 \end{bmatrix} \begin{bmatrix} \delta_{mx} \\ \delta_{my} \end{bmatrix} = \begin{bmatrix} \Phi_{m1} \\ \Phi_{m2} \end{bmatrix} \quad (20)$$

is solved for each antenna element to get its position $(\delta_{mx}, \delta_{my})$. The above procedure is repeated for every antenna element to find all positions δ_m .

3 Simulation Results

A simulation was done using parameters from a UAV flight over a LOFAR low-band antenna (LBA) outer sub-station consisting of 48 dipole antennas. A cross-scan flight is performed within a 100×100 m square at an altitude of approximately 100 m. From the cross-scan we can use $\phi_1 = 45^\circ$ and $\phi_2 = 135^\circ$ which leads to orthogonal directions Δ_1 and Δ_2 when viewing the flight path from above. Figure 2 illustrates the layout of the sub-station.

The UAV transmits the 5th, 7th, 9th, and 11th harmonics of a base frequency $f_0 = 6.3585$ MHz, thus $i = [2, 3, 4, 5]$. The largest absolute distances from the origin $|\delta_{mx}|$ and $|\delta_{my}|$ of all elements in the sub-station is about 60 m. The wavelength at the base frequency is $\lambda_0 = 47.1483$ m, therefore the conditions in (8) are not met. To allow for recovery from aliasing, let $\omega_v = \omega_0/4$ and $\sigma = 5$, to meet the conditions in (10). This gives us $\theta_\sigma = 38.7^\circ$. Let

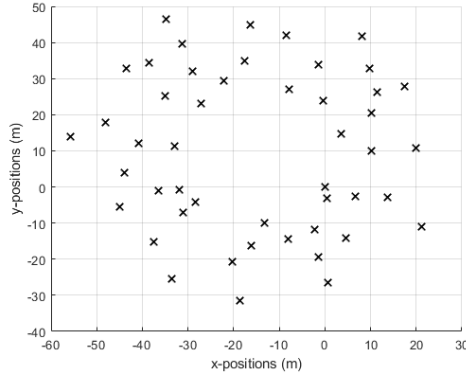


Figure 2. Antenna elements in an LBA outer sub-station.

$\rho = 7$ so that $\theta_{p_i} = [77.2^\circ, 61^\circ, 55^\circ, 51.6^\circ]$ at the different frequency harmonics ω_i .

The effect of noise on the system was evaluated from 100 Monte Carlo runs for each noise level from 15 – 50 dB in steps of 5 dB. The amount of snapshots $N_t = 80$ and the sub-snapshots used to evaluate Root-MUSIC is $N_s = 0.5N_t$. The RMS errors calculated for the x - and y -positions of the antenna elements are shown in Figure 3.

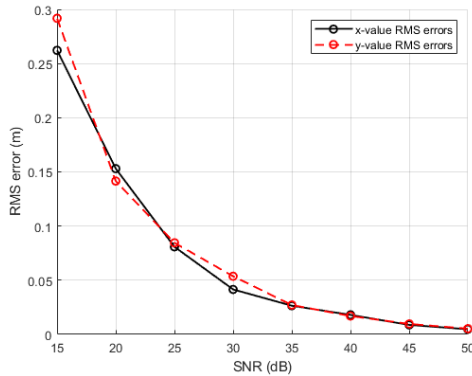


Figure 3. Root mean square errors of element positions in a LOFAR LBA outer sub-station for different noise levels. $N_t = 80$, $N_s = 0.5N_t$.

At an SNR of 15 dB, the RMS error is close to 30 cm for both x - and y -positions. This quickly drops down to errors around 5 cm at 30 dB. The results of Figure 3 prove that the proposed method works in the case of a controlled simulation. Further experiments are being done to understand the influence that various practical effects can have on the results.

4 Conclusion

In this paper, it is shown how the validated exponential analysis technique, VEXPA, can be used to estimate the positions of elements in an antenna array using harmonically related input signals transmitted from a UAV. The UAV's position in the sky is exploited to create a model that allows

recovery from aliasing. The effectiveness of the method has been illustrated by evaluation of the results for varied noise levels. The next step is to prove that the method works when using practical data from the field. Work in this regard is currently ongoing.

5 Acknowledgements

This work is based on the research supported in part by the National Research Foundation of South Africa (Grant Number 75322). It is also supported by the Netherlands Organisation for Scientific Research.

References

- [1] M.P. van Haarlem et al., "LOFAR: The Low Frequency Array", *Astronomy & Astrophysics*, **556**, A2, August 2013, pp. 1–53, doi: 10.1051/0004-6361/201220873
- [2] P. E. Dewdney, P. J. Hall, R. T. Schilizzi, and T. J. L. W. Lazio, "The Square Kilometre Array," *Proceedings of the IEEE*, **97**, 8, August 2009, pp. 1482–1496, doi: 10.1109/JPROC.2009.2021005.
- [3] S. J. Wijnholds, G. Pupillo, P. Bolli, and G. Virone, "UAV-Aided Calibration for Commissioning of Phased Array Radio Telescopes," in *URSI Asia-Pacific Radio Science Conference (URSI AP-RASC)*, 2016, pp. 228–231, doi: 10.1109/URSIAP-RASC.2016.7601375.
- [4] F. Knaepkens, A. Cuyt, W.-s. Lee and D. I. L. de Villiers, "Regular Sparse Array Direction of Arrival Estimation in One Dimension," in *IEEE Transactions on Antennas and Propagation*, **68**, 5, May 2020, pp. 3997–4006, doi: 10.1109/TAP.2019.2963618.
- [5] A. Cuyt, Y. Hou, F. Knaepkens and W.-s. Lee, "Sparse Multidimensional Exponential Analysis with an Application to Radar Imaging," *SIAM Journal on Scientific Computing*, **42**, 3, 2020, pp. B675–B695, doi:10.1137/19M1278004.
- [6] M. Briani, A. Cuyt, F. Knaepkens, and W.-s. Lee, "VEXPA: Validated EXPonential Analysis through Regular Sub-Sampling," *Signal Processing*, **177**, December 2020, doi:10.1016/j.sigpro.2020.107722.
- [7] A. Vesa, "Direction of Arrival Estimation Using MUSIC and Root-MUSIC algorithm," in *18th Telecommunications Forum*, 2010, pp. 582–585
- [8] A. Cuyt and W.-s. Lee, "How to get high resolution results from sparse and coarsely sampled data," *Applied and Computational Harmonic Analysis*, **48**, 3, 2020, pp. 1066–1087, doi: 10.1016/j.acha.2018.10.001.